

Sub-harmonic Oscillations in Power Circuits with Series Capacitors

By

Shigenori HAYASHI* and Akira KISHIMA*

(Received September 28, 1964)

A method based on the dual-input describing function is presented for the analysis of the sub-harmonic resonance of the order $1/3$ in the electric circuits containing one saturable reactor.

The paper describes the use of this method to analyse the $1/3$ -harmonic resonance which may be encountered in the application of series capacitors to power circuits, and presents the conditions on the circuit parameters to ensure the absence of the $1/3$ -harmonic resonance. An analog computer study on this problem is included.

1. Introduction

In recent years there has been a growing tendency to make use of series capacitors in order to improve the conditions on distribution and transmission lines. Along with the desirable characteristics of series capacitors, there results possible occurrence of undesirable phenomena¹⁾. One of these phenomena is "sub-harmonic resonance". This may occur when an unloaded or lightly loaded transformer is energized, or when a transformer is suddenly lightly loaded. Such operation may result in the abnormally large and badly distorted exciting currents in steady state as well as transient state, whose lowest-frequency is a sub-multiple of the source frequency. This peculiar circuit behavior depends essentially on the non-linear characteristic of the transformer. This type of circuit with a saturable reactor in series with a capacitor, has been investigated by many authors. However, so far as the authors know, the papers which have dealt analytically with the problem of sub-harmonic resonance in the power circuits with series capacitors are few. Hence, it is of importance to establish conditions between the parameters of the circuits in order to exclude such a phenomenon. In this paper, the circuit under consideration is, for brevity, assumed as a single-phase circuit, for which an equivalent circuit is established and investigated, since it may be guessed that

* Department of Electrical Engineering II

such an assumption might not give fatal errors. The range of the abnormal phenomena is determined by means of the dual-input describing function method introduced by J. C. West and J. L. Douce^{2,3}). The feature of the application of this method to the study of sub-harmonic resonance in power circuits is characterized by its simplicity and generality in analysis. In numerical calculations of power circuits, it is usually very convenient to work with dimensionless quantities and with magnitudes of the order of unity, viz., the per-unit system. The per-unit system is very attractive here, since it reduces the variables to dimensionless quantities expressed in decimal form and delivers the parameters into limited range. This analytical procedure can be similarly applied in the case of the sub-harmonic oscillation of the order $1/(2m+1)$; $m=1, 2, \dots$. But this paper deals only with the sub-harmonic oscillation of the order $1/3$ exclusively which may commonly be encountered in the application of series capacitors to power circuits.

2. Analytical Method

(a) Circuit Equation

The basic electric circuit considered is shown in Fig. 2.1, and consists of linear passive network, a saturable reactor and a driving voltage source. The equation for this circuit in terms of the electromotive force, e , the reactor current, i , and the flux linkage, ψ , is

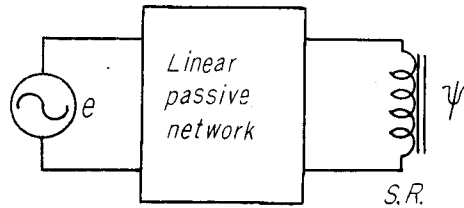


Fig. 2.1

$$\psi = \frac{M(p)}{p} \{e - Z(p)i\}, \quad i = f(\psi) \quad (2.1)$$

where $f(\psi)$ represents the non-linearity of the reactor and p is the time-derivative operator. Moreover, $M(p)$ and $Z(p)$ can be obtained in terms of the open- or the short-circuited impedances of the network. Let the electromotive force be of the form

$$e = E \cos(\omega t + \theta_0) \quad (2.2)$$

where E , ω and θ_0 are constants.

The basic assumptions for the circuit in the treatment are that the frequency response of $M(p)Z(p)/p$ falls with increasing frequency and that the function $f(\psi)$ is a single-valued and odd function of ψ .

(b) Periodic Solution and Describing Function

For the sub-harmonic oscillation whose fundamental frequency is a fraction 1/3 of that of the electromotive force given by Eq. (2.2), the periodic solution of Eq. (2.1) may be written as

$$\psi = a \cos(\omega t + \varphi) + b \cos \frac{1}{3} \omega t \quad (2.3)$$

where a is the amplitude of the fundamental component, b , that of the 1/3-harmonic component and φ is the phase angle between them. Substitute Eq. (2.3) into Eq. (2.1) and equate the coefficients of the fundamental and the 1/3-harmonic components respectively. Then it follows that

$$a \left\{ N(1) + \frac{j\omega}{M(j\omega)Z(j\omega)} \right\} = \frac{E}{Z(j\omega)} e^{j(\theta_0 - \varphi)} \quad (2.4)$$

$$N(\frac{1}{3}) = \xi_1 + j\eta_1 \quad (2.5)$$

where

$$\xi_1 + j\eta_1 = \left\{ -\frac{b}{M(p)Z(p)} \right\}_{p=j(\omega/3)} \quad (2.6)$$

$N(1)$ and $N(\frac{1}{3})$ introduced above are, respectively, the fundamental frequency and the 1/3-harmonic frequency describing functions for the non-linear characteristic $f(\psi)$. (See Appendix I) They are expressed by

$$N(1) = \frac{1}{a} \frac{2}{\pi} \int_0^\pi f\{a \cos(3\tau + \varphi) + b \cos \tau\} \varepsilon^{-j(3\tau + \varphi)} d\tau \quad (2.7)$$

$$N(\frac{1}{3}) = \frac{1}{b} \frac{2}{\pi} \int_0^\pi f\{a \cos(3\tau + \varphi) + b \cos \tau\} \varepsilon^{-j\tau} d\tau \quad (2.8)$$

Eq. (2.5) is now recognized to be the relationship that must exist between $\xi_1 + j\eta_1$ and $N(\frac{1}{3})$ for the generation of the 1/3-harmonic oscillation. The right-hand side of Eq. (2.5) is given by Eq. (2.6) and depends on the parameters of the linear network and on the order of the sub-harmonic considered. The left-hand side of Eq. (2.5) is given by Eq. (2.8) and depends on the non-linear characteristic of the reactor, on the amplitude of the fundamental and the 1/3-harmonic components of the flux linkage, on the phase angle between them and on the order of the sub-harmonic considered. As the phase angle φ is varied, the 1/3-harmonic frequency describing function $N(\frac{1}{3})$ plotted on the complex plane follows a closed curve symmetrical with respect to the real axis, since the function $f(\psi)$ is a single-valued odd function as assumed above. Such curves on the complex plane can be obtained for various values of a and b . As will be shown, these loci will be responsible for the occurrence of 1/3-harmonic resonance.

(c) $\frac{1}{3}$ -harmonic Frequency Describing Function Loci for Specific Non-linearities

(i) Consider the cubic non-linearity

$$f(\psi) = \psi^3 \quad (2.9)$$

By use of Eq. (2.8), $N(\frac{1}{3})$ is found to be

$$N(\frac{1}{3}) = \frac{3}{4}(2a^2 + b^2) + \frac{3}{4}ab\epsilon^{j\varphi} \quad (2.10)$$

As φ is varied, both the real and imaginary parts of this function vary. The locus plotted on the complex plane is a circle with center at $3(2a^2 + b^2)/4 + j0$ and a radius of $3ab/4$. By letting u = real part and v = imaginary part, it may be expressed by

$$\left\{u - \frac{3}{4}(2a^2 + b^2)\right\}^2 + v^2 = \left(\frac{3}{4}ab\right)^2 \quad (2.11)$$

Here, if a is maintained constant and b is varied, these describing function loci always lie in the area bounded by the following parabola.

$$v^2 = \frac{3}{4}a^2\left(u - \frac{21}{16}a^2\right) \quad (2.12)$$

This parabola is an envelope of the circles expressed by Eq. (2.11). Further, if a and b are both varied, the describing function loci always lie in the area bounded by the following lines.

$$v = \pm \frac{1}{\sqrt{7}}u; \quad u > 0 \quad (2.13)$$

This line is also an envelope of the parabolas expressed by Eq. (2.12).

(ii) Consider the non-linearity given by

$$f(\psi) = \psi^3 \quad (2.14)$$

In this case, $N(\frac{1}{3})$ can be evaluated as shown in Appendix II. Fig. 2.2 shows the plots of $N(\frac{1}{3})/a^3$ on the complex plane for several values of b/a . As for the cubic characteristic it is now possible to evaluate the describing function loci and to obtain the boundary curves when a is maintained constant and b is varied, or when a and b are both varied.

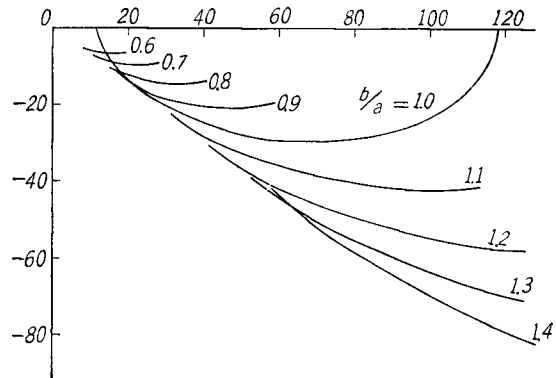


Fig. 2.2

(iii) Consider the non-linear characteristic defined by

$$f(\psi) = \begin{cases} \psi - \psi_0 & ; \psi > \psi_0 \\ 0 & ; |\psi| \leq \psi_0 \\ \psi + \psi_0 & ; \psi < -\psi_0 \end{cases} \quad (2.15)$$

where ψ_0 is a positive constant. In this case also, it is possible to calculate the describing function loci and to obtain the boundary curves. In Fig. 2.3, those are plotted on the complex plane for several values of ψ_0/a and b/a .

(iv) Finally consider the non-linear characteristic expressed by

$$f(\psi) = c_1\psi + c_0f_0(\psi) \quad (2.16)$$

where c_1 and c_0 are constants. The describing function loci and their boundary curves for $c_0f_0(\psi)$ can be obtained by multiplying those for $f_0(\psi)$ by c_0 . Thus, the describing function loci and their boundary curves for $f(\psi)$ can be obtained by shifting those for $c_0f_0(\psi)$ by c_1 parallel to the real axis. For example, consider a simple case where the non-linear characteristic is given by

$$f(\psi) = c_1\psi + c_0\psi^3 \quad (2.17)$$

The describing function locus and the boundary curves are given by

$$\left\{ (u - c_1) - c_0 \frac{3}{4} (2a^2 + b^2) \right\}^2 + v^2 = \left(c_0 \frac{3}{4} ab \right)^2 \quad (2.18)$$

$$v^2 = c_0 \frac{3}{4} a^2 \left\{ (u - c_1) - c_0 \frac{21}{16} a^2 \right\} \quad (2.19)$$

$$v = \pm \frac{1}{\sqrt{7}} (u - c_1) \quad (2.20)$$

Eqs. (2.18), (2.19) and (2.20) are corresponding to Eqs. (2.11), (2.12) and (2.13) respectively.

(d) Mechanism of $\frac{1}{3}$ -harmonic Generation

Again, return to Eq. (2.5). As seen above, the left-hand side of Eq. (2.5), viz., the describing function always lies in a certain region on the complex plane. If the amplitudes of the electromotive force would be varied arbitrarily, this region depends on the non-linear characteristic only. However, it is practical to determine the region from a knowledge of the operating values of the electromotive force and then of a and b . Although these operating values are also related by Eq. (2.4), it is frequently possible to assume the approximate values for them which will be satisfactory for use in calculations. The per-unit system used in power system analysis achieve this approximation. Thus, the relevant region to the operating conditions can be

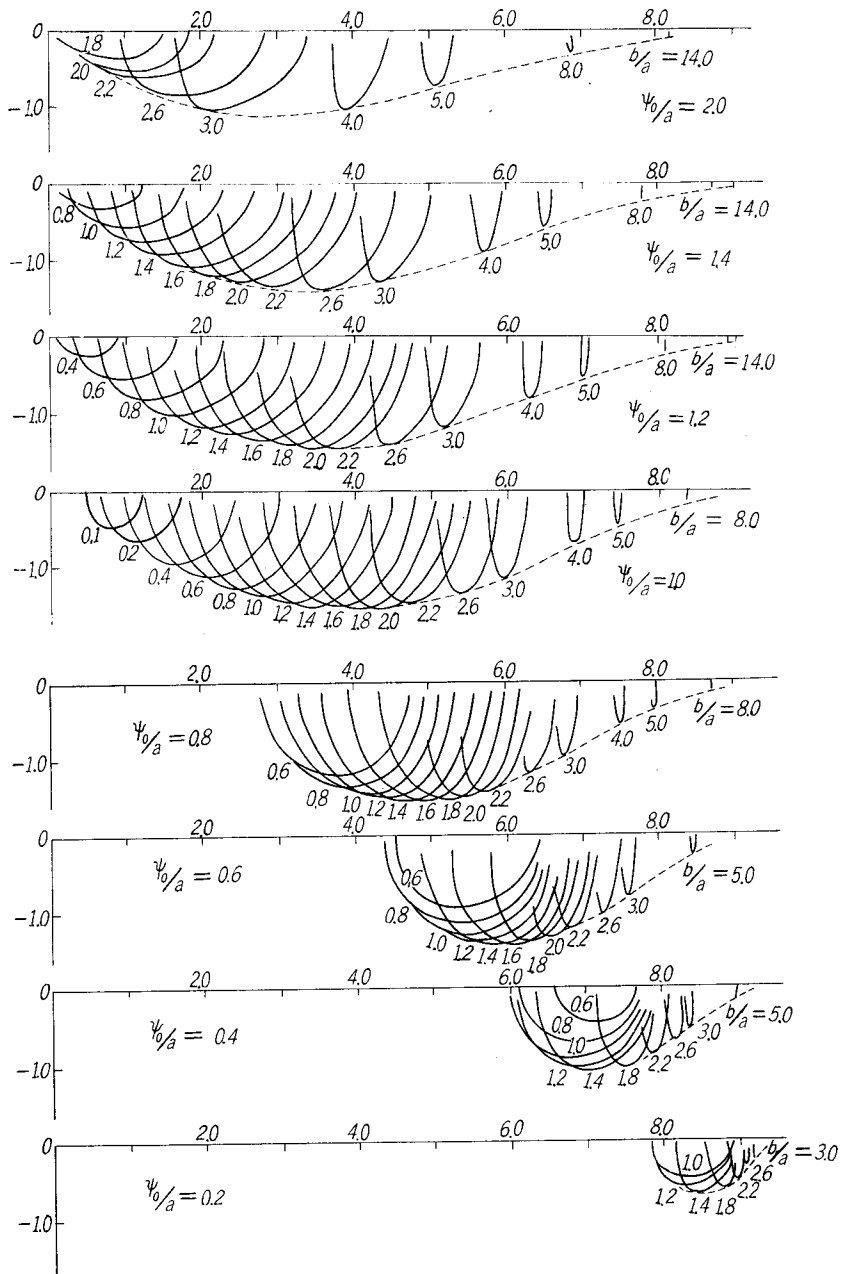


Fig. 2.3

determined. Therefore, it is possible to set up a criterion that if the point $\xi_1 + j\eta_1$ lies outside the relevant region, the 1/3-harmonic resonance will not be observed for the operating values considered.

(e) Condition for Stability

In order to investigate the stability of the evaluated periodic solution given by Eq. (2.3), it is necessary to consider the variational equation of Eq. (2.2)⁴. Let the small variation from the periodic solution of the flux linkage, ψ_s , be denoted by $\Delta\psi$. From Eq. (2.1), the variational equation becomes

$$\Delta\psi = -\frac{M(p)}{p}Z(p)f'(\psi_s)\Delta\psi \quad (2.21)$$

where $f'(\psi_s) = \{df/d\psi\}_{\psi=\psi_s}$. This differential equation with variable coefficients cannot easily be solved. However, the stability of the solution of this equation may be determined approximately by use of the describing function for $f'(\psi_s)\Delta\psi$. (See Appendix III)

3. Application to Power Circuits with Series Capacitors

The method developed so far can be quite readily applied to the 1/3-harmonic resonance in the power circuits with series capacitors, if the single-phase-approximation may be adopted. In this case, the exciting characteristic of a transformer corresponds to the non-linear characteristic of the reactor considered in the preceding, and $M(p)Z(p)$ in Eq. (2.6) is the operational impedance of the circuit viewed from the transformer terminals. In calculation, the per-unit system based on the kVA and the voltage ratings of the transformer is used throughout the power circuits considered.

(a) Relevant Regions for Transformers

The shape of the saturation curve of a transformer may vary considerably depending upon the grade of steel and the transformer design. The saturation curves used in this study are shown in Fig. 3.1. These curves give the value of the flux linkage and the exciting current in terms of the normal flux linkage and the normal current (not the normal exciting current) respectively. Unit flux linkage $\psi = 1.0$

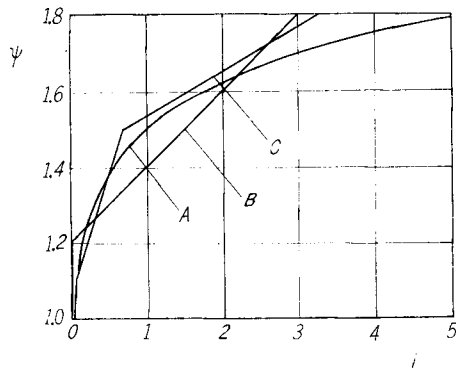


Fig. 3.1

defines the normal operating point on the saturation curves. Moreover, curves A and B in Fig. 3.1 are given by

$$i = 0.025\psi^3 \quad (3.1)$$

and

$$i = \begin{cases} 5(\psi - 1.2) & ; \psi > 1.2 \\ 0 & ; |\psi| \leq 1.2 \\ 5(\psi + 1.2) & ; \psi < -1.2 \end{cases} \quad (3.2)$$

respectively.

Now, from a practical viewpoint, assume that the amplitude of the fundamental frequency component of the flux linkage lies between 0.8 and 1.2. Then, the relevant region in this case can be determined by the use of the results described in the preceding section. Fig. 3.2 shows the boundary curves

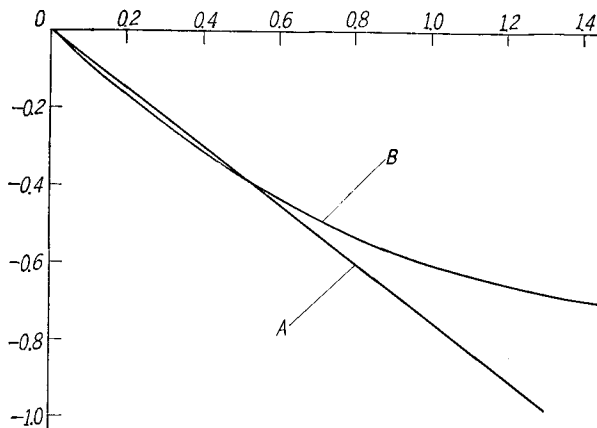


Fig. 3.2

obtained from the values shown in Fig. 2.2 and Fig. 2.3. Curves A and B in Fig. 3.2 correspond to curves A and B in Fig. 3.1, viz., Eq. (3.1) and Eq. (3.2) respectively.

(b) Unloaded Transformer

Consider a circuit with an unloaded transformer. The single-phase equivalent circuit analysed shown in Fig. 3.3, where r and x_l are the resistance and the inductive reactance of the line respectively and x_c is the capacitive reactance of

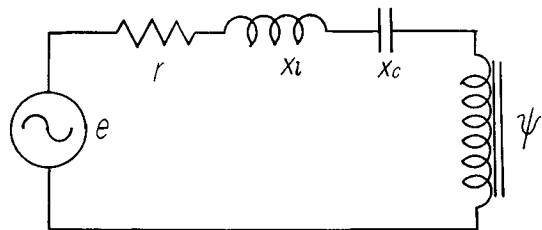


Fig. 3.3

the series capacitor. In order to obtain $\xi_1 + j\eta_1$, it is necessary to replace $M(p)Z(p)$ in Eq. (2.6) by its operational expression in terms of circuit parameters. In this case, it follows that

$$\left\{ -\frac{p}{M(p)Z(p)} \right\}_{p=j(\omega/3)} = \left\{ -\frac{P^2}{x_l P^2 + rP + x_c} \right\}_{P=j(1/3)} \quad (3.3)$$

Hence

$$\left. \begin{aligned} \xi_1 &= \frac{1}{9} \frac{x_c - \frac{1}{9}x_l}{\left(x_c - \frac{1}{9}x_l\right)^2 + \left(\frac{1}{3}r\right)^2} \\ \eta_1 &= -\frac{1}{9} \frac{\frac{1}{3}r}{\left(x_c - \frac{1}{9}x_l\right)^2 + \left(\frac{1}{3}r\right)^2} \end{aligned} \right\} \quad (3.4)$$

An interesting feature which may be noticed here is that as r is maintained constant and $9x_c - x_l$ is varied, $\xi_1 + j\eta_1$ plotted on the complex plane follows a circle with center at a point on the imaginary axis and as $9x_c - x_l$ is maintained constant and r is varied, $\xi_1 + j\eta_1$ follows a circle with center at a point on the real axis. Thus, if $\xi_1 + j\eta_1$ lies outside the region whose boundary curves are shown in Fig. 3.2, the 1/3-harmonic resonance will not be observed. The results of calculations shown in Figs. 3.4 (A) and (B) are obtained for the

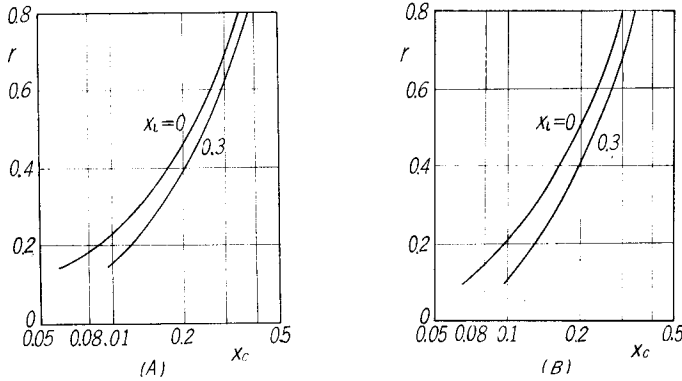


Fig. 3.4

saturation curves A and B in Fig. 3.1 respectively. In these figures, the region above each curve represents a non-resonant condition for the 1/3-harmonic oscillation.

(c) Loaded Transformer

The circuit has an impedance shunting the saturable reactor, simulating a load being taken off the circuit. The single-phase equivalent circuit to be

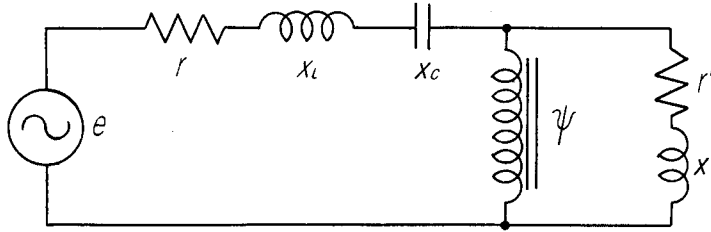


Fig. 3.5

analysed is shown in Fig. 3.5, where r' and x' are the resistance and the inductive reactance of the load respectively. In this case

$$\left\{ -\frac{p}{M(p)Z(p)} \right\}_{p=j(\omega/3)} = \left\{ -\frac{P(x_l+x')P^2+(r+r')P+x_c}{(x_lP^2+rP+x_c)(x'P+r')} \right\}_{P=j(1/3)} \quad (3.5)$$

Hence

$$\left. \begin{aligned} \xi_1 &= \frac{1}{9} \frac{x_c - \frac{1}{9}x_l}{\left(x_c - \frac{1}{9}x_l\right)^2 + \left(\frac{1}{3}r\right)^2} - \frac{1}{3} \frac{1}{z} \frac{\frac{1}{3}\sin\sigma}{\cos^2\sigma + \frac{1}{9}\sin^2\sigma} \\ \eta_1 &= -\frac{1}{9} \frac{\frac{1}{3}r}{\left(x_c - \frac{1}{9}x_l\right)^2 + \left(\frac{1}{3}r\right)^2} - \frac{1}{3} \frac{1}{z} \frac{\cos\sigma}{\cos^2\sigma + \frac{1}{9}\sin^2\sigma} \end{aligned} \right\} \quad (3.6)$$

where

$$z \cos \sigma = r', \quad z \sin \sigma = x' \quad (3.7)$$

It is interesting to point out that the first terms of the right-hand side of Eq. (3.6) are the same as the right-hand side of Eq. (3.4) and the second terms depend on the load parameters only. This relation on the complex plane is illustrated in Fig. 3.6, where the points P and P_0 , are given by Eqs. (3.6) and (3.4) respectively, and the distance vector of P for the loaded condition from P_0 for the unloaded is given by

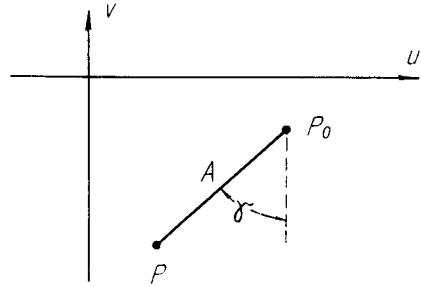


Fig. 3.6

$$\left. \begin{aligned} A &= \frac{1}{3z\sqrt{\cos^2\sigma + \frac{1}{9}\sin^2\sigma}} \\ \tan \gamma &= \frac{\tan \sigma}{3} \end{aligned} \right\} \quad (3.8)$$

From these results and the region shown in Fig. 3.2, the conditions on the circuit parameters to ensure the absence of the $1/3$ -harmonic resonance are

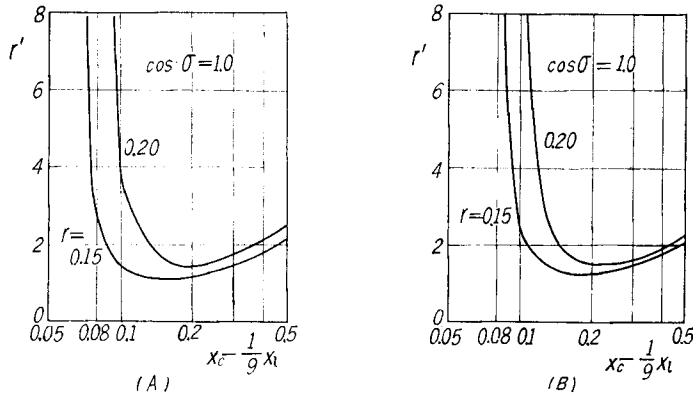


Fig. 3.7

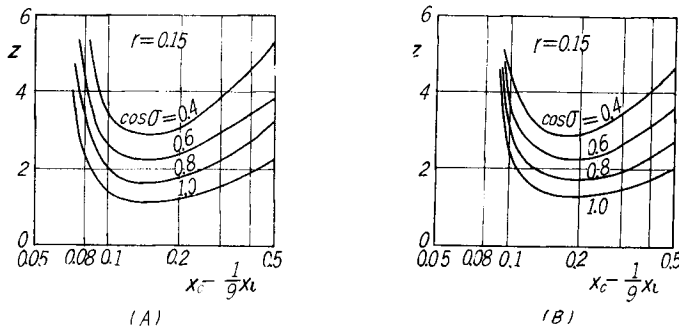


Fig. 3.8

derived. The calculated results for the resistive and the inductive loads are shown in Figs. 3.7 and 3.8 respectively, where (A) and (B) are also corresponding to the saturation curves A and B in Fig. 3.1 respectively, and the region below each curve represents a non-resonant condition for the 1/3-harmonic oscillation.

4. Analog Computer Study

An analog computer is used to obtain the solutions of the non-linear circuits analysed in the preceding section. The saturation curve used in this study is curve C in Fig. 3.1, and the electromotive force is applied at the zero point of the wave. The regions of the 1/3-harmonic resonance of the circuits shown in Figs. 3.3 and 3.5 are defined in terms of the circuit parameters and the applied voltage E where E is the per-unit voltage.

The computing results for the circuit shown in Fig. 3.3 are given in Fig. 4.1 and typical waveforms when a 1/3-harmonic oscillation occurs is shown

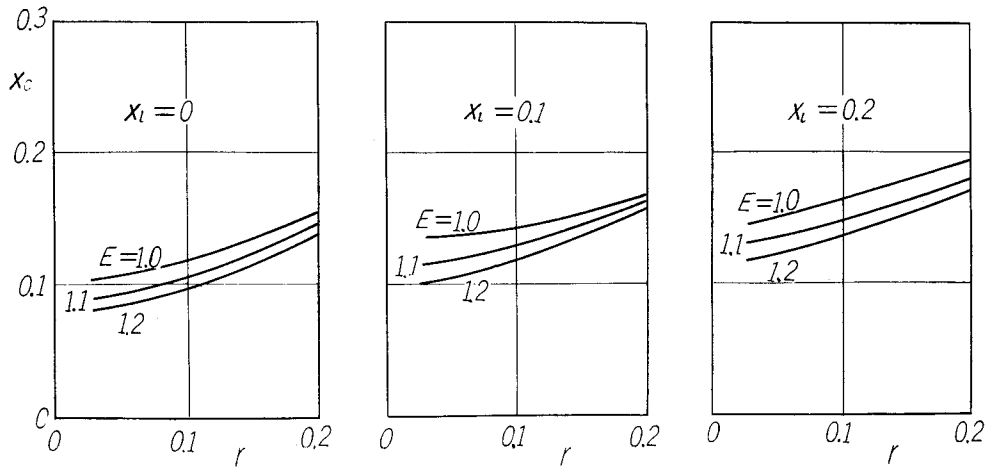


Fig. 4.1

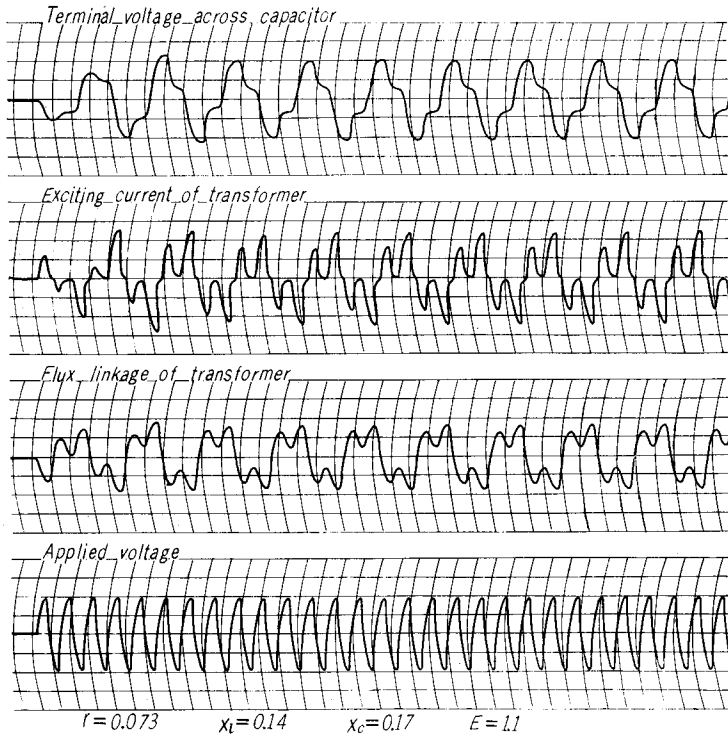


Fig. 4.2

in Fig. 4.2. In Fig. 4.1, the 1/3-harmonic resonance may occur in the region above each curve. In this case, smaller resistance results in an almost periodic or a non-periodic oscillation and larger capacitive reactance results in a sub-harmonic oscillation of the order 1/2. Next, the computing results for the circuit shown in Fig. 3.5 are given in Fig. 4.3, where the region above each curve is also that in which 1/3-harmonic resonance may occur.

The results in this study are in considerably good agreement with those obtained in the preceding section.

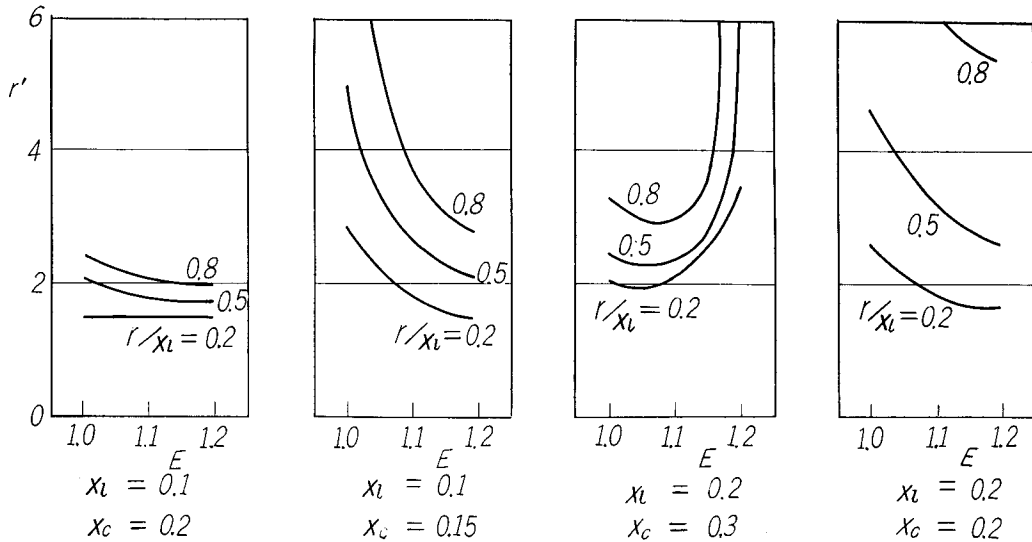


Fig. 4.3

5. Conclusion

A method has been presented giving a graphical analysis of generation of the 1/3-harmonic resonance in the electric circuits containing one saturable reactor. Such phenomena observed in the power circuits with series capacitors can be explained quantitatively by the method. The effect of the circuit parameters such as resistance and reactance on such phenomena are examined. The results obtained by the analog computer study indicate that the analytical method would be useful.

The stability of the 1/3-harmonic oscillations may be considered by use of a similar method. The method is readily applied in the so-called ferro-resonance in electric circuits.

Further work is proceeding on the analysis of the three-phase circuit with series capacitors where the 1/3-harmonic oscillations may occur.

Acknowledgment

The authors wish to express their cordial thanks to Mr. Tatsuji Urata for his invaluable assistance in the numerical calculations.

References

- 1) J. W. Butler and C. Concordia : E. E., **56**, 975 (1937).
- 2) J. C. West, and J. L. Douce : Proc. I. E. E., **102B**, 569 (1955).
- 3) J. C. West, J. L. Douce and R. K. Liversley : Proc. I. E. E., **103B**, 463 (1956).
- 4) C. Hayashi : "Forced Oscillation in Non-Linear Systems" Nippon Printing Co., Osaka (1953).

Appendix I

Consider an input given by

$$\psi = a \cos(\omega t + \varphi) + b \cos \frac{1}{3} \omega t \quad (\text{I. 1})$$

applied to the non-linear element expressed by

$$i = f(\psi) \quad (\text{I. 2})$$

Now, assume that the output for this input is approximately composed of the two components whose frequencies are the same as the input. Then the output may be written in the form

$$i = A \cos(\omega t + \varphi - \Phi) + B \cos\left(\frac{1}{3} \omega t - \Theta\right) \quad (\text{I. 3})$$

Then, the describing functions may be defined as

$$N(1) = \frac{A}{a} \varepsilon^{-j\Phi} \quad (\text{I. 4})$$

for the fundamental frequency component, and

$$N\left(\frac{1}{3}\right) = \frac{B}{b} \varepsilon^{-j\Theta} \quad (\text{I. 5})$$

for the 1/3-harmonic frequency component, respectively.

When function $f(\psi)$ is single-valued and odd, the describing functions defined by Eqs. (I. 4) and (I. 5) become

$$N(1) = \frac{1}{a} \frac{2}{\pi} \int_0^{\pi} f\{a \cos(3\tau + \varphi) + b \cos \tau\} \varepsilon^{-j(3\tau + \varphi)} d\tau \quad (\text{I. 6})$$

$$N\left(\frac{1}{3}\right) = \frac{1}{b} \frac{2}{\pi} \int_0^{\pi} f\{a \cos(3\tau + \varphi) + b \cos \tau\} \varepsilon^{-j\tau} d\tau \quad (\text{I. 7})$$

Eqs. (I. 6) and (I. 7) are the same as Eqs. (2. 7) and (2. 8) respectively.

Appendix II

Consider a specific non-linearity expressed by

$$f(\psi) = \psi^{2\nu+1}; \quad \nu = 1, 2, \dots \quad (\text{II. 1})$$

Then, the describing function for the sub-harmonic frequency component will be of the form

$$\begin{aligned} N\left(\frac{1}{2m+1}\right) &= \frac{1}{2^{2\nu}} \left\{ \sum_i \sum_{r=y_i}^{x_i} a^{2(\nu-r)+1} b^{2r-1} \binom{2\nu+1}{2r} \binom{2\nu-r+1}{x_i-r} \binom{2r}{r-y_i} \varepsilon^{j(2\nu-x_i+1)\varphi} \right. \\ &+ \sum_j \sum_{r=y_j}^{x_j} a^{2(\nu-r)+1} b^{2r-1} \binom{2\nu+1}{2r} \binom{2\nu-r+1}{x_j-r} \binom{2r}{r-y_j} \varepsilon^{-j(2\nu-x_j+1)\varphi} \\ &+ \left. \sum_k \sum_{r=y_k}^{x_k} a^{2r} b^{2(\nu-r)} \binom{2\nu+1}{2\nu-r+1} \binom{2\nu-r+1}{x_k-r} \binom{2r}{r-y_k} \varepsilon^{j2y_k\varphi} \right\} \end{aligned}$$

$$+ \sum_l \sum_{r=y_l}^{x_l} a^{2r} b^{2(\nu-r)} \left(\frac{2\nu+1}{2\nu-r+1} \right) \binom{2\nu-r+1}{x_l-r} \binom{2r}{r-y_l} \varepsilon^{-j2y_l\varphi} \} \quad (\text{II. 2})$$

Where x_i, y_i, \dots, x_l and y_l are zeros or integers and satisfy the following relations;

$$\left. \begin{aligned} y_i &= (2m+1)(\nu-x_i)+m & ; & \quad 0 \leq x_i \leq \nu, \quad 0 \leq y_i \leq x_i \\ y_j &= (2m+1)(\nu-x_j)+m+1 & ; & \quad 0 \leq x_j \leq \nu, \quad 0 \leq y_j \leq x_j \\ y_k &= (\nu-x_k+1)/(2m+1) & ; & \quad 0 \leq x_k \leq \nu, \quad 0 \leq y_k \leq x_k \\ y_l &= (\nu-x_l)/(2m+1) & ; & \quad 0 \leq x_l \leq \nu, \quad 0 \leq y_l \leq x_l \end{aligned} \right\} \quad (\text{II. 3})$$

m being integer.

Now, setting $m=1$ leads to the expression for the 1/3-harmonic frequency describing function. The results shown in Fig. 2.2 are calculated from this formula.

Appendix III

Consider the non-linearity expressed by $i=f(\psi)$ again.

The variational equation which shows the relationship between Δi , the incremental change in i and $\Delta\psi$, the incremental change in ψ in the region about $\psi=\psi_s$, becomes

$$\Delta i = f'(\psi_s) \Delta\psi \quad (\text{III. 1})$$

where $f'(\psi_s) = \{df/d\psi\}_{\psi=\psi_s}$.

If ψ_s is a periodic solution of Eq. (2.1) and is given by Eq. (2.3),

$$\psi_s = a \cos(\omega t + \varphi) + b \cos \frac{1}{3} \omega t, \quad (\text{III. 2})$$

the variational equation of Eq. (2.1) will be

$$\Delta\psi = -\frac{M(\dot{p})}{p} Z(\dot{p}) f'(\psi_s) \Delta\psi \quad (\text{III. 3})$$

For the stability study, $\Delta\psi$ may be approximately assumed to be in the form

$$\Delta\psi = \delta \cos \left(n \frac{1}{3} \omega t + \theta \right) \quad (\text{III. 4})$$

where δ is very small compared with a and b , and n is an arbitrary constant. Here, to consider the input $\Delta\psi$ given by Eq. (III.4) applied to the element whose output Δi to $\Delta\psi$ is given by Eq. (III.1), leads to the same concept as that described in Appendix I. Thus, the describing function for the incremental change, viz., the incremental describing function $N(\delta)$ can be defined. Then, it will be

$$\left. \begin{aligned} N(\delta) &= \frac{1}{\pi} \int_0^\pi f'(\psi_s) d\tau & ; & \quad n \neq \text{integer} \\ &= \frac{1}{\pi} \int_0^\pi f'(\psi_s) \{1 + \varepsilon^{-j2(n\tau+\theta)}\} d\tau & ; & \quad n = 1, 2, \dots \end{aligned} \right\} \quad (\text{III. 5})$$

It follows from Eq. (III. 5) that if n is an integer, $N(\delta)$ is a function of θ , an arbitrary phase angle which can be assumed to be any value from 0 to 2π , and its locus as θ is varied is a circle with center at $\left\{\frac{1}{\pi} \int_0^\pi f'(\psi_s) d\pi + j0\right\}$ and a radius of $\left[\left\{\frac{1}{\pi} \int_0^\pi f'(\psi_s) \cos 2n\tau d\tau\right\}^2 + \left\{\frac{1}{\pi} \int_0^\pi f'(\psi_s) \sin 2n\tau d\tau\right\}^2\right]^{1/2}$ on the complex plane.

On the other hand, by use of the incremental describing function, the characteristic equation for the stability may be written in the form

$$1 + \frac{M(p)}{p} Z(p) N(\delta) = 0 \quad (\text{III. 6})$$

This enables the Nyquist diagram to be plotted. Thus, since the original system is passive, it is possible to set up a criterion that if, for a certain value of n , the incremental describing function locus encloses the point $\xi_n + j\eta_n$ given by

$$\xi_n + j\eta_n = \left\{ -\frac{p}{M(p)Z(p)} \right\}_{p=jn(\omega/s)} ; \quad n = 1, 2, \dots, \quad (\text{III. 7})$$

any slight disturbance will initiate an oscillation of increasing amplitude, so that the periodic solution assumed initially is unstable. If n , the order of the unstable region, is even, it may give preferable results to add a constant term to the right-hand side of Eq. (III. 4).